Deletion of the GATA Domain of TRPS1 Causes an Absence of Facial Hair and Provides New Insights into the Bone Disorder in Inherited Tricho-Rhino-Phalangeal Syndromes

Talat H. Malik,[1,2,3,4] Dietrich von Stechow,[5,6] Roderick T. Bronson,[7]
and Ramesh A. Shivdasani[1,2,3,4]*

Departments of Medical Oncology[1] and Cancer Biology,[2] Dana-Farber Cancer Institute, Department of Medicine, Brigham and Women's Hospital,[3] Department of Orthopedic Surgery, Beth Israel Deaconess Medical Center,[5] and Departments of Medicine,[4] Surgery,[6] and Pathology,[7] Harvard Medical School, Boston, Massachusetts

GATA transcription factors mediate cell differentiation in diverse tissues, and their dysfunction is associated with certain congenital human disorders. The six classical vertebrate GATA proteins, GATA-1 to GATA-6, are highly homologous, bear two tandem zinc fingers of the C_4 (GATA) type, and activate transcription. TRPS1, the only other vertebrate protein with the GATA motif, is a large, multitype zinc finger protein that harbors a single DNA-binding GATA domain and represses transcription. Monoallelic *TRPS1* mutations cause two dominantly inherited human developmental disorders of the hair, face, and digits, tricho-rhino-phalangeal syndrome (TRPS) types I (MIM 190350) and III (MIM 190351); missense GATA domain mutations account for the more severe type III form. Here we report that heterozygous mice with deletions of the TRPS1 GATA domain (TRPS1$^{+/\Delta gt}$) display facial anomalies that overlap with findings for TRPS, whereas TRPS1$^{\Delta gt/\Delta gt}$ mice additionally reveal a complete absence of vibrissae. Unexpectedly, TRPS1$^{\Delta gt/\Delta gt}$ mice die of neonatal respiratory failure resulting from abnormalities of the thoracic spine and ribs. Heterozygotes also develop thoracic kyphoscoliosis with age and reveal structural deficits in cortical and trabecular bones. These findings directly implicate the GATA type zinc finger of TRPS1 in regulation of bone and hair development and suggest that skeletal abnormalities emphasized in descriptions of TRPS are only the extreme manifestations of a generalized bone dysplasia.

GATA transcription factors are defined by the presence of zinc finger motifs with the consensus sequence $CXNCX_{17}CNXC$ and execute essential functions in vertebrate and invertebrate development. The C_2C_2 GATA-type zinc finger binds the consensus DNA sequence WGATAR found in the control regions of many developmentally regulated and tissue-specific genes. The six well-characterized vertebrate GATA factors are highly homologous and conserved, contain two GATA-type zinc fingers, and activate transcription. GATA1, -2, and -3 regulate key aspects of blood or neural cell differentiation (36, 42, 44, 52, 55), whereas GATA4, -5, and -6 cooordinate a variety of developmental processes in the endoderm and heart (20, 22, 23, 32, 45). In lower metazoans GATA proteins carry a single canonical zinc finger, as exemplified by *Caenorhabditis elegans* END-1 and *Drosophila* PANNIER/dGATAa, which are required in endoderm and proneural development, respectively (13, 62). GATA proteins appear to function as the obligate DNA-binding components of multiprotein complexes that may include FOG-1, FOG-2, or P300/CBP in vertebrates (1, 18, 50, 51, 56) and U-SHAPED in *Drosophila melanogaster* (5). However, the abundance of GATA sequences in regulatory *cis* elements suggests that developmental control of lineage-restricted genes probably involves additional layers of complexity.

TRPS1 is a recently described vertebrate nuclear protein with nine predicted zinc finger domains, including a single carboxyl-terminal GATA-type zinc finger (27, 33). Besides the GATA motif, homology with other proteins is limited to two C-terminal zinc fingers closely related to a domain found in the Ikaros family of lymphoid transcription factors (8). In contrast to other vertebrate GATA proteins, TRPS1 behaves as a potent, sequence-specific transcriptional repressor in vitro and in vivo; the repression function maps to the Ikaros domain (27). Thus, TRPS1 is a unique and atypical vertebrate GATA factor.

Monoallelic mutations in human *TRPS1* cause the tricho-rhino-phalangeal syndromes (TRPS) (33), dominantly inherited conditions characterized by developmental defects of the hair, face, and selected bones (11). Patients with TRPS have a bulbous nose, a long and flat philtrum, a thin upper lip, sparse scalp hair that grows slowly, and, occasionally, protruding ears (9, 11). The sum of these findings attests to a requirement for TRPS1 in specific aspects of hair growth regulation and facial morphogenesis. Besides the cosmetic defects in facial soft tissues, patients classically show cone-shaped epiphyses, usually confined to the middle or proximal phalangeal bones of the hands and feet, and, less commonly, premature closure of the growth plate in other tubular bones. Various hip malformations are frequently detected when they are sought (6, 11, 25), consistent with expression of *TRPS1* mRNA in the developing femoral head (27). In type III TRPS (MIM 190351), which is most commonly caused by missense mutations in the TRPS1 GATA domain (25), there is severe brachydactyly and short stature resulting from generalized and progressive shortening of all phalanges and metacarpals as well as some long bones

* Corresponding author. Mailing address: Dana-Farber Cancer Institute, 1 Jimmy Fund Way, Boston, MA 02115. Phone: (617) 632-5746. Fax: (617) 632-5739. E-mail: ramesh_shivdasani@dfci.harvard.edu.

(17). Some authors have therefore speculated that TRPS may reflect general disorders of bone development (6, 12). This is a difficult question to address with regard to patients, who show wide phenotypic variation, even within affected families (6, 11, 16, 25), and for whom clinical description is often incomplete.

To investigate the role of the TRPS1 GATA-type zinc finger in mammalian development, we generated mice with targeted deletions of the GATA motif ($TRPS1^{\Delta gt}$), and here we report the mutant phenotypes. Besides a superficial overlap between clinical findings in human TRPS and $TRPS1^{\Delta gt}$ mutant mice, homozygotes reveal several unexpected abnormalities, including a complete absence of vibrissae and neonatal death from respiratory failure. Investigation of the latter finding revealed its basis in a general defect in skeletal development, with powerful correlates in adult heterozygote mice. Our observations thus indicate that the requirement for the GATA domain of TRPS1 is not limited to bones in the extremities, as is strongly implied in the clinical literature, but extends to skeletal development in general. These findings provide a faithful animal model for a human developmental disorder and extend the understanding of *TRPS1* gene function in development and disease.

MATERIALS AND METHODS

Gene targeting and generation and genotyping of $TRPS1^{\Delta gt}$ mice. *TRPS1* genomic fragments were isolated from a strain 129-derived λ phage library (Stratagene). *Bam*HI/*Sal*I fragments (3.1 kb) and *Sal*I/*Not*I fragments (2.8 kb) flanking exon IV were cloned into the 5′ and 3′ homology sites, respectively, of the modified gene targeting vector pPNT6 (57) to replace a 3.8-kb region with the PGK-*neo*^{R} cassette flanked by LoxP recognition sites (47). J1 embryonic stem (ES) cells (2) were electroporated with the targeting construct and selected in G418 and ganciclovir. Homologous recombinant ES cell clones were identified by Southern analysis of *Bam*HI- or *Kpn*I-digested genomic DNA using flanking 5′ or 3′ probes, respectively. These probes were amplified by PCR with the primer pair 5′-GGCCATGGGAAGTTGTGTATT-3′ and 5′-CAAGTGGCTT AACATTCAGAG-3′ and the primer pair 5′-GAAGTTGGGAGAACAAATA GGA-3′ and 5′-TCCTCTCAGATTGCCCTCTTTA-3′, respectively. $TRPS1^{\Delta gt}$ mutant mice were generated independently on mixed genetic backgrounds between the 129/Sv, C57BL/6, and BALB/c strains, and we observed no phenotypic differences across strains. Littermates served as controls in all experiments.

Reverse transcriptase PCR (RT-PCR). Total RNA was extracted from $TRPS1^{+/\Delta gt}$ newborn kidney in Trizol reagent (Life Technologies) and reverse transcribed using oligo(dT) primers. Specific primers used to amplify the region surrounding nucleotides encoding the GATA-type zinc finger were 5′-GACTC TGAGGGACAGCCCCAAT-3′ and 5′-GTCAATGAACCCTGGGCTTCG-3′.

Analysis of neonatal mice. Neonatal mice were sacrificed by methoxyflurane inhalation before showing clinical signs of respiratory distress. For histologic analysis, samples were treated overnight in Bouin's fixative, dehydrated in a graded ethanol series, and embedded in paraffin. Sections (7 μm thick) were stained with hematoxylin and eosin and were examined by light microscopy. Skin samples from the back were fixed on filter paper to generate flat sections; individual hair follicles per microscopic field diameter were counted manually and averaged over at least 20 independent sections from several mice.

Glycogen staining. Slides were deparaffinized, rehydrated in distilled water, and treated sequentially with 1% periodic acid (5 min), Schiff reagent (20 min), and Harris's hematoxylin (1 min), with a 5- to 10-min wash in distilled water between each step.

Electron microscopy. Lungs were freshly dissected from live newborn mice before onset of labored breathing and were fixed overnight in Karnovsky's fixative (2.5% paraformaldehyde, 2% glutaraldehyde, 0.2 M cacodylate buffer [pH 7.2]) at 4°C. Samples were postfixed in osmium tetroxide, washed, dehydrated through an ascending series of alcohols, infiltrated with propylene oxide, and embedded in epoxy resin. Ultrathin sections were stained with uranyl acetate and lead citrate and were examined with a Philips 208S electron microscope at an accelerating voltage of 60 kV.

Staining of cartilage and bone. Adult and neonatal mice were sacrificed by CO_2 or methoxyflurane inhalation, respectively. Skin and soft tissues were removed, and skeletons were fixed in 95% ethanol and stained with alcian blue and

alizarin red S as described previously (30). In situ hybridization analysis was performed as reported previously, by using separately two antisense riboprobes specific for mouse *TRPS1* (27).

Micro-CT analysis. Detailed 3-dimensional (3-D) evaluation of bones was performed on a desktop microcomputed tomography (micro-CT) system (μCT 20; Scanco Medical AG, Bassersdorf, Switzerland). Scans were acquired at 34-μm slice increments, and images were stored in 3-D arrays with an isotropic voxel size of 34 μm. A constrained 3-D Gaussian filter was used to suppress noise, and mineralized and soft tissues were segmented by a global thresholding procedure (35). Morphometric parameters were determined by using a direct 3-D approach (15) in three different preselected femoral regions: whole bone (including articular ends), secondary spongiosa in the distal metaphysis, and diaphyseal cortex.

RESULTS

Targeted deletion of the GATA domain from mouse TRPS1. The presence of a single GATA motif in TRPS1 raises important questions about its evolutionary significance and specific role in development. We deleted the fourth coding exon in the mouse gene (27), which encodes only the GATA-type zinc finger and 15 additional amino acids required for DNA binding (40). To avoid unintended consequences for transcription from the *TRPS1* gene locus, the neomycin resistance cassette in the targeting vector (Fig. 1a) was flanked by LoxP sites, which permitted generation of the Δ*gt* allele. Subsequently, we mated $TRPS1^{\Delta gt}$ heterozygotes with transgenic mice that express Cre recombinase widely in early development (29) in order to generate a distinct Δ*neogt* allele lacking the selection cassette. Correctly targeted ES cells, recognized by predicted Southern blot patterns (Fig. 1b), were used to produce chimeric mice and, subsequently, $TRPS1^{\Delta gt}$ and $TRPS1^{\Delta neogt}$ heterozygotes. RT-PCR on kidneys of $TRPS1^{+/\Delta gt}$ fetuses amplified two discrete *TRPS1* transcripts (Fig. 1c), and sequencing of the mutant PCR product verified in-frame loss of nucleotides encoding amino acids 888 to 928; this reflects targeted deletion of the GATA-type zinc finger with preservation of the dominant nuclear localization signal (residues 946 to 952).

$TRPS1^{\Delta gt}$ and $TRPS1^{\Delta neogt}$ mice show the same phenotypes. Heterozygote matings produce $TRPS1^{\Delta gt/\Delta gt}$ and $TRPS1^{\Delta neogt/\Delta neogt}$ mice in the expected numbers until late gestation (Table 1), but homozygotes uniformly die within 6 h of birth after presenting evidence of initial respiratory and feeding efforts (Fig. 2a). We attribute the sub-Mendelian ratio of homozygotes in the neonatal period to maternal cannibalism of pups that die especially early.

Hair and facial abnormalities in $TRPS1^{\Delta gt}$ mutant mice overlap with findings in human TRPS. A single defective allele is sufficient to cause human TRPS (33), and only one patient is reported with putative homozygous mutations (25). In contrast, the spectrum of developmental defects that overlaps with clinical findings in humans is different in $TRPS1^{+/\Delta gt}$ and $TRPS1^{\Delta gt/\Delta gt}$ mice. Homozygous, but not heterozygous, mutant $TRPS1^{\Delta gt}$ mice conspicuously lack vibrissae (Fig. 2b and c), the specialized sensory hairs normally found in characteristic arrays along the upper jaw. Whiskers are absent in $TRPS1^{\Delta gt/\Delta gt}$ mice throughout late gestation, except for scattered atretic follicles (Fig. 2c), and there is no histologic indication that more follicles are formed earlier but subsequently regress. The $TRPS1^{\Delta gt}$ allele is also associated with a general defect in pelage hair development: the average number of hair follicles present per unit length of dorsal skin surface is reduced by
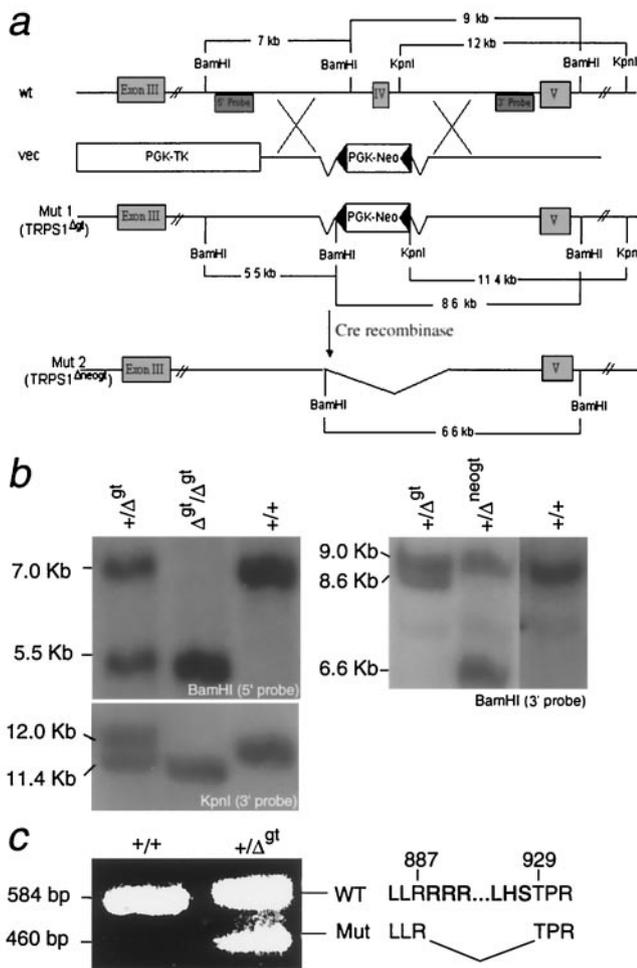
FIG. 1. Targeted disruption of the GATA domain in the mouse *TRPS1* gene. (a) Gene targeting strategy for replacement of coding exon IV with a PGK-Neo[r] cassette flanked by *LoxP* sequences (left-pointing triangles). The targeting construct (vec) also contained a thymidine kinase (PGK-TK) cassette for counterselection. Locations of the 5′ and 3′ flanking probes used in Southern analysis and predicted band sizes in *Bam*HI- and *Kpn*I-digested DNA for the wild-type (wt) and targeted (Mut1, *TRPS1*$^{\Delta gt}$; Mut2, *TRPS1*$^{\Delta neogt}$) alleles are indicated. (b) Southern blot detection of *TRPS1* alleles in wild-type (+/+), heterozygote (+/Δgt and +/$\Delta neogt$), and homozygous null (Δgt/Δgt) mice. (c) RT-PCR analysis of fetal kidney mRNA confirms expression of the two predicted *TRPS1* transcripts. The mutated product shows in-frame deletion of nucleotides encoding amino acid residues 888 to 928.

almost 50% in newborn *TRPS1*$^{\Delta gt/\Delta gt}$ mice, and there is an intermediate number in *TRPS1*$^{+/\Delta gt}$ neonates (Fig. 3a and b). However, unlike in human TRPS, where hair loss is progressive after birth (16, 49), defects in quantitative or qualitative aspects of the pelage are not evident in adult *TRPS1*$^{\Delta gt}$ heterozygotes. Hair follicle development and maintenance depend on complex, bidirectional interactions between the skin and its underlying mesenchyme (31, 41), and *TRPS1* mRNA is prominently expressed throughout the mesenchyme of the developing anterior facies (27). In this regard, we further note the virtual absence of ventral, nonsensory hairs along the mandible in *TRPS1*$^{\Delta gt/\Delta gt}$ neonates (Fig. 2c).

Some features of human TRPS, often subtle in patients, are

TABLE 1. Representation of each *TRPS1* genotype in mice during fetal life and at birth

Age[a]	No. of mice			
	+/+	+/Δgt	Δgt/Δgt	Total
E12	2	4	1	7
E15	3	7	5	15
E18	15	34	20	69
P0	45	97	27	169

[a] E, embryonic day; P0, day of birth.

predictably difficult to ascertain in mice. The lengths of the philtrum and selected phalanges, which are always abnormal in patients but often undetected in youth (10), are not measurably affected in *TRPS1*$^{+/\Delta gt}$ mice up to the age of 6 months (Fig. 3c; also data not shown). In contrast, anomalies of the chin and palate that have been described for a number of patients (12, 16) are readily recognized in *TRPS1*$^{\Delta gt/\Delta gt}$ neo-
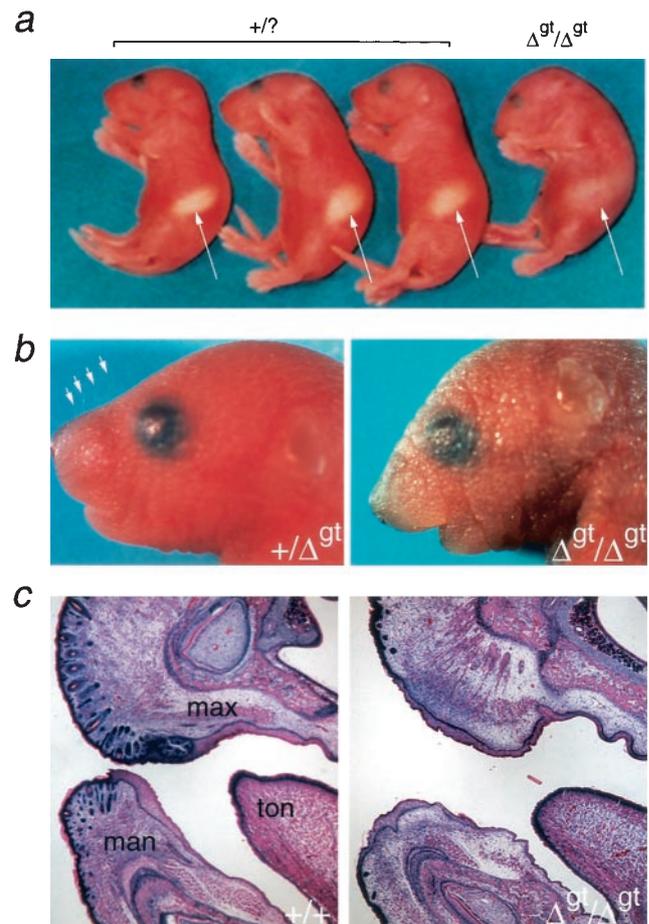

FIG. 2. Mortality and lack of vibrissae in homozygous *TRPS1*$^{\Delta gt}$ mutant mice. (a) Gross appearance of a homozygous mutant neonate (Δgt/Δgt) shortly before death, compared to control littermates (+/?), indicating successful early respiration and feeding (arrows point to milk in the stomach). Note the hunched posture of the homozygous mutant. (b) Facial close-up showing absence of vibrissae in *TRPS1*$^{\Delta gt/\Delta gt}$ mice. (c) Tissue sections showing only rare atretic follicles in the anterior facies in *TRPS1*$^{\Delta gt/\Delta gt}$ mice. max, maxilla; man, mandible; ton, tongue.
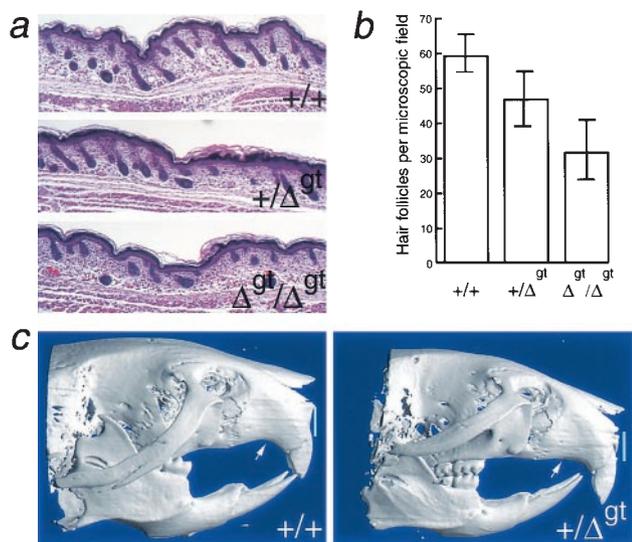
FIG. 3. Hair and craniofacial anomalies with loss of the TRPS1 GATA domain. (a) Histology of representative sections of dorsal skin from newborn wild-type, heterozygous, and homozygous mutant mice. (b) Average counts of hair follicles per diameter of the microscopic field visible with the $4\times$ lens objective ($n = 20$ for each genotype), showing progressive reduction in follicle density with mutations in each gene copy. (c) Skeletal reconstructions from micro-CT of the adult head, highlighting (arrows) the abnormal palatal arch seen in 10 consecutive mice, without alteration in the width of the bony region corresponding to the human philtrum (bars).

nates and $TRPS1^{+/\Delta gt}$ adults, in the form of micrognathia (a small, recessed chin [Fig. 2b]) and an abnormally arched (but not cleft) palate (Fig. 3c), respectively. Thus, the Δgt allele of mouse $TRPS1$ fairly reproduces the human disease phenotype; the lack of a perfect overlap may reflect either species differences or the essential, modular functions of peptide domains other than the GATA-type zinc finger.

Unexpected neonatal mortality of homozygous $TRPS1^{\Delta gt/\Delta gt}$ mice. Although the findings described above highlight the requirement for the TRPS1 GATA domain in selected aspects of facial and hair development, they do not readily explain why mutant homozygotes die in the neonatal period. After breathing normally for as long as 6 h, $TRPS1^{\Delta gt/\Delta gt}$ mice develop progressively labored respiratory effort and cyanosis, and die of visible respiratory failure. Visceral histologic defects in full necropsy specimens are confined to the lung parenchyma, and other sites of $TRPS1$ mRNA expression (kidneys, brain, and gut) are unaffected. Because postmortem pulmonary abnormalities may be evident in mice that die of nonrespiratory causes, we were particularly careful about making this distinction. Even in mice sacrificed immediately after birth, well before the onset of labored breathing, the lungs reveal reduced air spaces and markedly thickened septae (Fig. 4a and b). Consistent with the clinical evidence for respiratory failure, glycogen deposits, normally nearly absent from the newborn respiratory epithelium (28), are considerably retained in the $TRPS1^{\Delta gt/\Delta gt}$ lung parenchyma (Fig. 4c and d). Morphological defects are restricted to the distal respiratory epithelium,
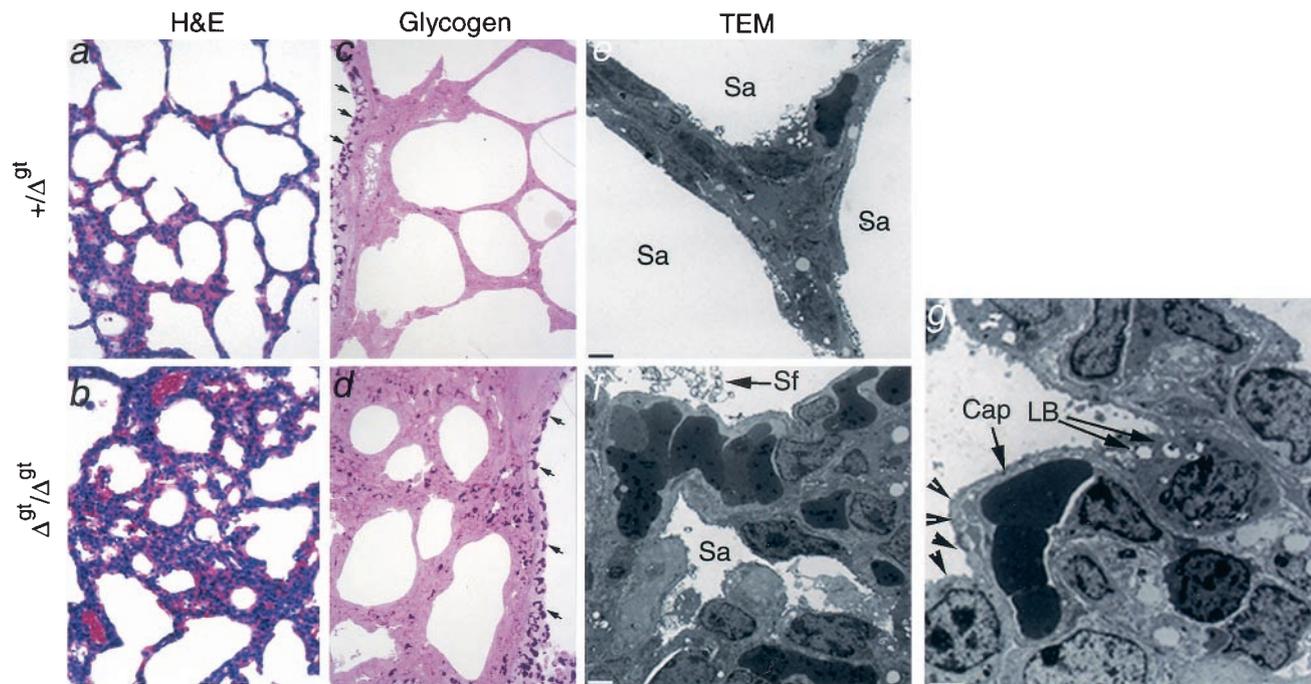

FIG. 4. Pulmonary histopathology in newborn $TRPS1^{\Delta gt/\Delta gt}$ mice. In comparison to heterozygote littermates (a and c), homozygous mutants sacrificed even before signs of overt respiratory failure show poorly inflated lungs (b) in tissue sections stained with hematoxylin and eosin (H&E) and retention of fetal glycogen in the distal respiratory epithelium (d). Arrows in panels c and d point to cytoplasmic glycogen in the columnar (bronchial) epithelium, which is normal. Differences in the expansion of lung saccules (Sa) are highlighted in transmission electron microscopic (TEM) analysis (e and f), which also shows abundant tubular myelin forms of pulmonary surfactant (Sf) in prospective mutant alveoli (f). Bars, 2 μm. (g) High-resolution TEM (bar, 0.5 μm) further reveals intracellular multilamellar bodies (LB) in mutant type II pneumocytes and formation of suitable gas exchange surfaces between the cytoplasm of type I pneumocytes (arrowheads) and pulmonary capillaries (Cap).

whereas lung mass and lobularity, in vitro branching morphogenesis, and appearance of the large conducting airways are normal (Fig. 4; also data not shown). Ultrastructural analysis indicates that lung saccules fail to expand properly despite the presence of alveolar surfactant (Fig. 4e and f).

Neonatal respiratory failure can result from primary lung developmental defects or from secondary causes (14), and several independent observations suggest a nonpulmonary basis for lung atelectasis in $TRPS1^{\Delta gt/\Delta gt}$ mice. First, newborn mice initially appear healthy, oxygenate normally as indicated by their pink color, and feed (Fig. 2a). Second, fetal lung fluid is cleared and the epithelial maturation markers thyroid transcription factor 1, hepatocyte nuclear factor 3β, and surfactant proteins A through C are all expressed in the normal distribution (data not shown). Third, type II pneumocytes harbor numerous cytoplasmic multilamellar bodies (Fig. 4g) and produce abundant tubular myelin forms of alveolar surfactant (Fig. 4f), findings that exclude a major category of neonatal primary pulmonary dysfunction (4). Fourth, ultrastructure reveals the membranes of type I pneumocytes closely apposed to functioning capillaries (Fig. 4g), indicating proper formation of a gas-exchange interface. Finally, $TRPS1$ mRNA levels are considerably lower in wild-type fetal or neonatal lungs than in other visceral and skeletal sites (data not shown), which argues against a cell-autonomous role in lung development per se. The weight of evidence hence suggests a mechanical basis for respiratory failure; fetal epithelial glycogen is often retained in this setting (14, 28).

Skeletal abnormalities as the basis for mechanical respiratory failure. $TRPS1^{\Delta gt/\Delta gt}$ mice show no evidence of neurologic compromise or histologic defects in the diaphragm or trachea (data not shown) as possible reasons for respiratory failure. Rather, examination of the neonatal skeleton reveals a striking degree of spinal scoliosis (Fig. 5a), consistent with a grossly evident postural abnormality (Fig. 2a). This uniform defect is associated with a rib cage that is reduced in size and curves inward at the base (Fig. 5a). Endochondral ossification is delayed, both in the ribs, which are thin and abnormally curved (Fig. 5b), and throughout the vertebral column, as illustrated for the cervical spine (Fig. 5c). To determine if the sites of skeletal pathology correlate with those of $TRPS1$ expression, we performed in situ hybridization. Although $TRPS1$ mRNA is predominantly expressed in the snout and femur in midgestation (27), the next-highest expression is indeed detected in developing vertebral bodies and ribs (Fig. 5d), the same structures that are anatomically and functionally compromised in homozygous mutant mice. Combined with the clinical and pathological evidence for respiratory failure, these findings suggest a scenario wherein structural thoracic defects compromise inspiratory function and lead to pulmonary atelectasis and progressive respiratory compromise in $TRPS1^{\Delta gt/\Delta gt}$ mice. Similar skeletal defects serve as the basis for respiratory neonatal lethality in a variety of engineered mouse strains (2, 39, 46, 60) and in human syndromes of severe dwarfism and skeletal dysplasia (14, 53).

Generalized skeletal defects in $TRPS1^{\Delta gt}$ mutant mice. These findings, unexpected from the clinical manifestations emphasized in human TRPS, prompted us to examine $TRPS1^{+/\Delta gt}$ mice in closer detail. We observed a substantial degree of kyphoscoliosis in the spines of 11 of 12 $TRPS1^{+/\Delta gt}$
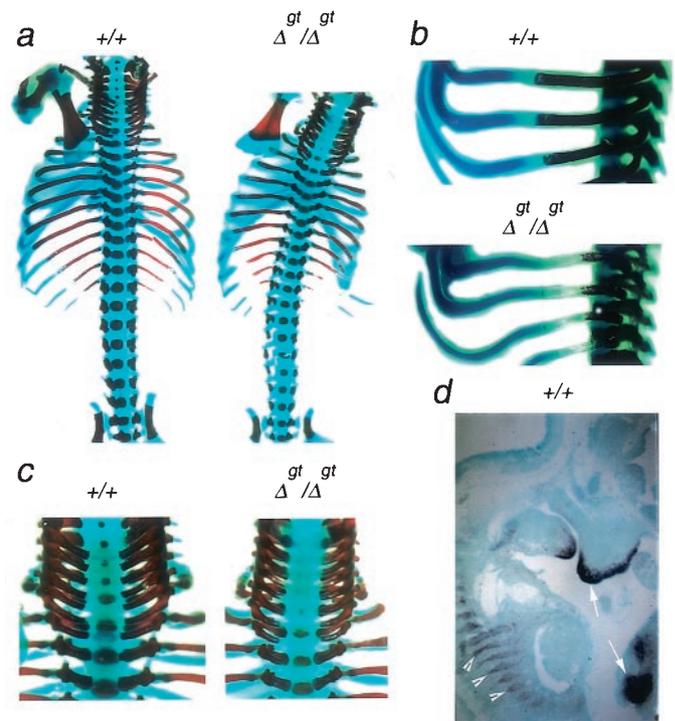

FIG. 5. Skeletal abnormalities in the absence of the TRPS1 GATA domain. (a) Wild-type (left) and $TRPS1^{\Delta gt/\Delta gt}$ (right) newborn skeletons stained with alcian blue and alizarin red, showing dramatic spinal scoliosis and reduced thoracic cage volume in homozygous mutants. (b and c) Close-up views of ribs 5 to 7 (b) and the cervical spine (c) further reveal reduced bone development (alizarin red staining) and extreme curvature of the cartilaginous rib component. (d) In situ hybridization analysis of wild-type midgestation mouse fetus showing $TRPS1$ mRNA expression in developing vertebrae and ribs (arrowheads), albeit at lower levels than in the anterior facial mesenchyme and developing femur (arrows).

heterozygotes by the age of 3 months (Fig. 6a), although this was not associated with overt postural or respiratory defects. TRPS1 is hence necessary for proper skeletal function in varied locations, and to investigate the nature of this requirement, we obtained detailed morphometric information using quantitative micro-CT. Femurs from 10 adult $TRPS1^{+/\Delta gt}$ female mice revealed significant reductions in whole (63.5% ± 1.7% versus 67.1% ± 1.0% in wild-type littermates [$P < 0.001$]) and especially trabecular (0.81% ± 0.47% versus 1.9% ± 0.6% in wild-type littermates [$P < 0.01$]) bone volume density, and this quantitative defect is reflected in the morphology of trabecular bone (Fig. 6c). Other measurable bone parameters were largely unperturbed, as were the size and morphology of the femoral body, head, and neck (Fig. 6b). Our findings thus indicate that two intact copies of the $TRPS1$ gene are necessary for proper development of mammalian trabecular bone in particular and that this function depends on the GATA-type zinc finger domain.

DISCUSSION

GATA proteins regulate tissue-specific gene transcription and have unique functions in development. In mice, deletion of individual $GATA$ genes causes a panoply of lethal developmen-
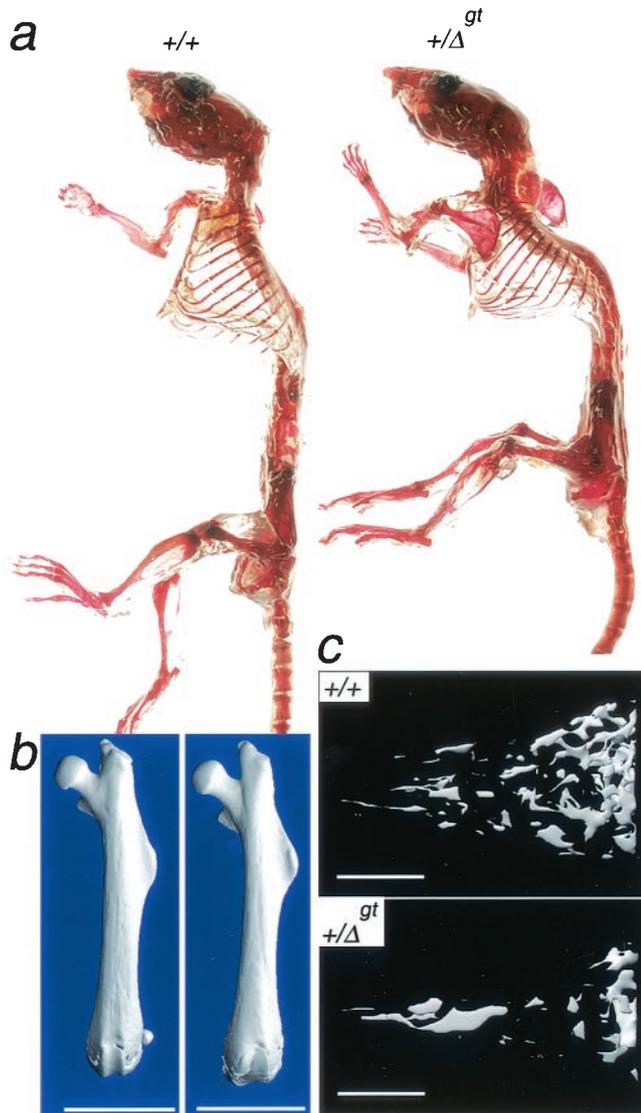
FIG. 6. Structural bony defects in adult *TRPS1*$^{+/\Delta gt}$ mice. (a) Wild-type (left) and heterozygous mutant (right) adult (3-month-old) skeletons stained with alcian blue and alizarin red, showing severe kyphoscoliosis with altered contour of the thoracic cavity in heterozygotes, findings that were confirmed radiographically (data not shown) for 9 of 10 adults. (b) Skeletal reconstructions of the whole femur from adult wild-type (left) and *TRPS1*$^{+/\Delta gt}$ (right) mice, showing preservation of the morphology and anatomic relationships of the shaft, head, and neck. Bars, 5 mm. (c) Three-dimensional reconstructions from micro-CT of distal femoral metaphyseal trabecular bone from representative adult (3-month-old) females, indicating reduced trabecular bone volume density in *TRPS1*$^{+/\Delta gt}$ heterozygotes. Bars, 1 mm.

tal defects, including hematopoietic arrest (44, 48, 52, 55), neural, urogenital, ventral body wall, and cardiac defects (22, 24, 32, 36, 37, 42, 61), or blocked endoderm differentiation and lung branching morphogenesis (19, 20, 34). Attesting further to the importance of GATA transcription factors in development, deficiencies of GATA1 (7, 38), GATA3 (58), and possibly GATA4 (43) result in congenital defects in differentiation of human blood cells, parathyroid glands, and kidneys and heart, respectively. It is therefore important to scrutinize GATA-

dependent transcriptional pathways and to understand how they might interact with other regulatory factors.

Among vertebrate GATA proteins, TRPS1 has unique evolutionary, structural, and functional properties. Whereas the classical GATA factors, GATA1 to -6, are structurally homologous and even substitute for each other in some contexts (3, 54), TRPS1 harbors a single, DNA-binding GATA-type zinc finger and shares no additional homology with the other GATA factors. It binds DNA with the same apparent preference for the WGATAR consensus sequence but antagonizes GATA-dependent gene activation in cultured mammalian cells and *Xenopus* embryos (27). Therefore, in principle, TRPS1 functions could intersect with those of other GATA proteins or could be largely independent. *TRPS1* mRNA is expressed widely, albeit at different levels, in fetal and adult tissues (33). Developmental expression is highest in sites most obviously affected in TRPS (27) and does not clearly overlap with or complement the expression patterns of other GATA factors (T. H. Malik and R. A. Shivdasani, unpublished data). Considered together, these findings suggest two general possibilities: either TRPS1 has isolated requirements in proper development of only those tissues affected in TRPS or it plays a role broader than that evidenced in the human syndromes. The latter possibility is underscored by the finding that affected individuals carry one wild-type *TRPS1* allele and are therefore informative only for the heterozygous state.

We used targeted gene disruption to delete the exon encoding the GATA-type zinc finger from the murine *TRPS1* gene. This strategy allows genetic focus on the questions outlined above and receives support from the observation that point mutations confined to the GATA domain cause a severe form of isolated TRPS, type III (25). Moreover, disrupting the GATA motif prevents DNA binding and sequence-specific transcriptional repression in vitro (27). In contrast, there is presently little insight into the unique functions of the large, complex N terminus of TRPS1, and our study does not address its role directly. The phenotypes identified in *TRPS1*$^{\Delta gt}$ mice are not reminiscent of functions attributed to other GATA factors, and the developmental expression patterns are not similar (Malik and Shivdasani, unpublished), so the notion that TRPS1 may directly antagonize GATA transcriptional activators in vivo seems unlikely. Instead, TRPS1 has unique essential developmental functions, consistent with its ancient evolutionary origin (27). Besides anomalies that mimic features of human TRPS, including reduced hair density and facial morphogenetic defects, *TRPS1*$^{\Delta gt}$ mutant mice have unexpected defects that serve to illuminate the role of TRPS1 in development and disease.

Before discussing these functions, it is worth comparing the spectrum of findings in humans and mice, which do not strictly overlap. The cosmetic features of TRPS probably result from abnormal morphogenesis of soft tissues, such as the upper lip, philtrum, and tip of the nose, and the human data are descriptive rather than quantitative. Corresponding defects, if present in *TRPS1*$^{\Delta gt}$ mutant mice, are difficult to ascertain conclusively, and doing so will not provide fresh insights. In contrast, the abnormally arched palate seen in all *TRPS1*$^{\Delta gt}$ heterozygotes and the small, recessed chin in mutant homozygotes must reflect species-independent morphogenetic functions for TRPS1 at the site of highest expression in fetal life (27). *TRPS1* poly-

morphisms may also contribute to phenotypic heterogeneity of facial features.

In further contrast to human TRPS, where brachydactyly is a defining feature, $TRPS1^{\Delta gt}$ heterozygotes do not show the same overt defect. The molecular nature of underlying mutations cannot explain this discrepancy, because patients with isolated GATA domain mutations that might resemble the $TRPS1^{\Delta gt}$ allele have severe brachydactyly (25). More likely, the small size of mouse phalanges precludes detection of subtle changes, especially when they are not associated with syndactyly or other gross anomalies. Accordingly, we carefully assessed the femur, a site of frequent pathology in TRPS (11) and of high $TRPS1$ mRNA expression in development (26). Although the femur in $TRPS1^{+/\Delta gt}$ mice shows distinct trabecular bone defects, it does not develop abnormalities of the femoral head described in TRPS. One possibility is that the pathology in humans reflects weight bearing, which is not a main function of the hip in quadripeds; indeed, hip abnormalities typically develop later in life than does brachydactyly in TRPS (16). Alternatively, the lack of detectable hip pathology in $TRPS1^{\Delta gt}$ heterozygote mice may reflect species differences in discrete requirements for the GATA domain of TRPS1.

The lack of vibrissae and neonatal mortality from respiratory failure are two unexpected and informative defects that $TRPS1^{\Delta gt}$ mice display as homozygotes. The nearly complete absence of whisker hair follicles at any point in gestation indicates that mesenchymal induction of dermal placodes does not occur and that hair development is never initiated on the snout. Although the specialized hair follicles that generate vibrissae could simply be more dependent on intact TRPS1 function than those of other hair types, two considerations suggest a more complex scenario. First, $TRPS1^{\Delta gt}$ mutant mice and patients with TRPS both display a global quantitative hair follicle defect, suggesting that the whisker phenotype is extreme but not isolated. Second, even in the head in $TRPS1^{\Delta gt/\Delta gt}$ neonates, dramatic alopecia is not confined to vibrissa follicles but is also noted along the lower jaw (Fig. 3a). Thus, the anatomic distribution of severe alopecia correlates best with that of highest $TRPS1$ mRNA expression during development (27), and this expression in the facial mesenchyme is probably required to help generate signals that induce hair placode formation in the adjacent cutaneous epithelium.

The range of hair anomalies in TRPS patients, who always have sparse and fragile scalp and eyebrow hairs (11, 25), and $TRPS1^{\Delta gt}$ mutant mice suggests an additional role for TRPS1 in hair follicle morphogenesis. It has previously been shown that cells within dermal papillae in hair follicles also express $TRPS1$ mRNA (27); this expression may be essential for proper hair development at late stages, whereas mesenchymal TRPS1 is required independently to induce facial hair formation. Both processes are hence inferred to depend on genes regulated through GATA cis elements. Although initial development of vibrissae and of pelage hairs probably occurs through similar mechanisms, discordant morphogenesis of mammalian hair follicle subtypes has been described. Among mice engineered to address molecular mechanisms of hair development, $Lef1^{-/-}$ mice in particular show modest pelage defects and a complete absence of vibrissae (21, 59). In contrast, $TRPS1^{\Delta gt/\Delta gt}$ mice uniquely illustrate the regional loss of two distinct facial hair subtypes, and it is likely that related

mechanisms regulate the anatomic boundaries of hair development in many locations. Studying transcriptional targets of TRPS1 and how they influence signaling by the Wnt, hedgehog, bone morphogenetic protein, and other pathways will further advance the understanding of skin appendage development.

The most significant phenotype of $TRPS1^{\Delta gt}$ mutant mice is skeletal, consisting of prominent kyphoscoliosis in adult heterozygotes and axial skeletal abnormalities that cause lethal respiratory failure in newborn homozygotes. The most prominent feature in the latter is reduced (presumably delayed) endochondral ossification throughout the vertebral column and rib cage; consequently, individual ribs and the whole rib cage are abnormally shaped and fail to support inspiratory effort. These findings indicate that TRPS1 is required for proper bone development at each site where it is expressed at appreciable levels: phalanges of the hands and feet and the femoral head, as demonstrated in the human disease, and the axial skeleton, ribs, and femur, as evidenced in $TRPS1^{\Delta gt}$ mutant mice. Again, our findings directly implicate the GATA zinc finger motif in this essential function. The phenotype resembles features of lethal human skeletal dysplasias, including thanatophoric and campomelic dwarfism, and of mice with mutations in the $Myf-5$ or $MRF4$ gene, where congenital rib abnormalities cause perinatal respiratory mortality (2, 14, 39, 53). The specific skeletal defects in $TRPS1^{\Delta gt}$ homozygotes most closely resemble findings for mice with combined absence of the homeobox genes $Dlx5$ and $Dlx 6$ (46).

Individual case reports document a wide spectrum of skeletal defects in patients with TRPS, although many of these are frequently overlooked; radiographic evaluation is usually limited to the distal extremities and focused on the highly penetrant digital defects that originally defined the clinical syndrome. However, when sought, anomalies of the spine, including kyphoscoliosis, are also observed in patients with TRPS (6, 12, 16), and the mouse data suggest that these may represent a common, albeit subclinical, aspect of the disease phenotype. Although the axial skeletal defects are greatest in homozygous mutant mice, they are also present in heterozygotes, which are genetically more similar to TRPS patients. Clinical studies indicate that skeletal abnormalities in TRPS are not only progressive but also quite variable, even within families (6, 11, 16, 17, 25), so that modifier genes are likely to influence phenotypic severity. Nevertheless, the findings for $TRPS1^{\Delta gt}$ mutant mice establish bone homeostasis as an essential function of TRPS1 in vivo and suggest that skeletal defects may be more common in TRPS than has been appreciated to date.

Because inherited TRPS are associated with monoallelic $TRPS1$ mutations, Momeni et al. suggest that disease results from gene haploinsufficiency (33). However, mutations within the GATA or Ikaros type zinc finger domain (27), and possibly all truncating mutations identified in humans (25, 33), create alleles that can function as dominant antagonists of the wild-type protein (27). In the case of $TRPS1^{\Delta gt}$ mutant mice, one cannot distinguish conclusively between these two molecular mechanisms. Some defects seen in homozygotes, as in the axial skeleton and pelage, are more severe than similar defects in heterozygote mice, but $TRPS1^{+/\Delta gt}$ mice have no detectable abnormality in development or numbers of vibrissae. Hence, some developmental processes are more sensitive than others

to the gene dose of either wild-type *TRPS1* or inhibitory mutant forms lacking the GATA domain.

In summary, targeted gene disruption in mice highlights the central importance of the GATA motif in TRPS1 function, suggests that its role in mammalian development is independent of other GATA proteins, and sheds new light on human TRPS. We propose that a generalized skeletal dysplasia underlies the bone abnormalities reported in TRPS and that impaired development of trabecular bone is an important feature of the phenotype. Accordingly, further examination of the spine, rib cage, and other sites in affected kindreds will likely reveal widespread skeletal defects that are clinically silent.

REFERENCES

1. **Blobel, G. A., T. Nakajima, R. Eckner, M. Montminy, and S. H. Orkin.** 1998. CREB-binding protein cooperates with transcription factor GATA-1 and is required for erythroid differentiation. Proc. Natl. Acad. Sci. USA **95:**2061–2066.
2. **Braun, T., M. A. Rudnicki, H. H. Arnold, and R. Jaenisch.** 1992. Targeted inactivation of the muscle regulatory gene Myf-5 results in abnormal rib development and perinatal death. Cell **71:**369–382.
3. **Chang, A. N., A. B. Cantor, Y. Fujiwara, M. B. Lodish, S. Droho, J. D. Crispino, and S. H. Orkin.** 2002. GATA-factor dependence of the multitype zinc-finger protein FOG-1 for its essential role in megakaryopoiesis. Proc. Natl. Acad. Sci. USA **99:**9237–9242.
4. **Clark, J. C., S. E. Wert, C. J. Bachurski, M. T. Stahlman, B. R. Stripp, T. E. Weaver, and J. A. Whitsett.** 1995. Targeted disruption of the surfactant protein B gene disrupts surfactant homeostasis, causing respiratory failure in newborn mice. Proc. Natl. Acad. Sci. USA **92:**7794–7798.
5. **Cubadda, Y., P. Heitzler, R. P. Ray, M. Bourouis, P. Ramain, W. Gelbart, P. Simpson, and M. Haenlin.** 1997. *u-shaped* encodes a zinc finger protein that regulates the proneural genes *achaete* and *scute* during the formation of bristles in *Drosophila*. Genes Dev. **11:**3083–3095.
6. **Felman, A. H., and J. L. Frias.** 1977. The trichorhinophalangeal syndrome: study of 16 patients in one family. Am. J. Roentgenol. **129:**631–638.
7. **Freson, K., K. Devriendt, G. Matthijs, A. Van Hoof, R. De Vos, C. Thys, K. Minner, M. F. Hoylaerts, J. Vermylen, and C. Van Geet.** 2001. Platelet characteristics in patients with X-linked macrothrombocytopenia because of a novel GATA1 mutation. Blood **98:**85–92.
8. **Georgopoulos, K., S. Winandy, and N. Avitahl.** 1997. The role of the Ikaros gene in lymphocyte development and homeostasis. Annu. Rev. Immunol. **15:**155–176.
9. **Giedion, A.** 1966. Das tricho-rhino-phalangeale Syndrom. Helv. Paediatr. Acta **21:**475–485.
10. **Giedion, A.** 1998. Phalangeal cone-shaped epiphyses of the hand: their natural history, diagnostic sensitivity, and specificity in cartilage hair hypoplasia and the trichorhinophalangeal syndromes I and II. Pediatr. Radiol. **28:**751–758.
11. **Giedion, A., M. Burdea, Z. Fruchter, T. Meloni, and V. Trosc.** 1973. Autosomal-dominant transmission of the tricho-rhino-phalangeal syndrome. Report of 4 unrelated families, review of 60 cases. Helv. Paediatr. Acta **28:**249–259.
12. **Goodman, R. M., R. Trilling, M. Hertz, H. Horoszowski, P. Merlob, and S. Reisner.** 1981. New clinical observations in the trichorhinophalangeal syndrome. J. Craniofac. Genet. Dev. Biol. **1:**15–29.
13. **Haenlin, M., Y. Cubadda, F. Blondeau, P. Heitzler, Y. Lutz, P. Simpson, and P. Ramain.** 1997. Transcriptional activity of *pannier* is regulated negatively by heterodimerization of the GATA DNA-binding domain with a cofactor encoded by the *u-shaped* gene of *Drosophila*. Genes Dev. **11:**3096–3108.
14. **Harding, R., and C. Albuquerque.** 1999. Pulmonary hypoplasia: role of mechanical factors in prenatal lung growth, p. 364–394. *In* C. Gaultier, J. R. Bourbon, and M. Post (ed.), Lung development. Oxford University Press, New York, N.Y.
15. **Hildebrand, T., A. Laib, R. Muller, J. Dequeker, and P. Ruegsegger.** 1999. Direct three-dimensional morphometric analysis of human cancellous bone: microstructural data from spine, femur, iliac crest, and calcaneus. J. Bone Miner. Res. **14:**1167–1174.
16. **Howell, C. J., and R. Wynne-Davies.** 1986. The tricho-rhino-phalangeal syndrome. A report of 14 cases in 7 kindreds. J. Bone Joint Surg. Br. **68:**311–314.
17. **Kajii, T., I. Fernandez Gonzalez, and S. Matsuura.** 1994. Tricho-rhino-phalangeal syndrome type III. Am. J. Med. Genet. **49:**349–350.
18. **Kakita, T., K. Hasegawa, T. Morimoto, S. Kaburagi, H. Wada, and S. Sasayama.** 1999. p300 protein as a coactivator of GATA-5 in the transcription of cardiac-restricted atrial natriuretic factor gene. J. Biol. Chem. **274:**34096–34102.
19. **Keijzer, R., M. van Tuyl, C. Meijers, M. Post, D. Tibboel, F. Grosveld, and M. Koutsourakis.** 2001. The transcription factor GATA6 is essential for branching morphogenesis and epithelial cell differentiation during fetal pulmonary development. Development **128:**503–511.
20. **Koutsourakis, M., A. Langeveld, R. Patient, R. Beddington, and F. Grosveld.** 1999. The transcription factor GATA6 is essential for early extraembryonic development. Development **126:**723–732.
21. **Kratochwil, K., D. Maude, I. Farinas, J. Galceran, and R. Grosschedl.** 1996. Lef1 expression is activated by BMP-4 and regulates inductive tissue interactions in tooth and hair development. Genes Dev. **10:**1382–1394.
22. **Kuo, C. T., E. E. Morrisey, R. Anandappa, K. Sigrist, M. M. Lu, M. S. Parmacek, C. Soudais, and J. M. Leiden.** 1997. GATA4 transcription factor is required for ventral morphogenesis and heart tube formation. Genes Dev. **11:**1048–1060.
23. **Laverriere, A. C., C. MacNeill, C. Mueller, R. E. Poelmann, J. B. Burch, and T. Evans.** 1994. GATA-4/5/6, a subfamily of three transcription factors transcribed in developing heart and gut. J. Biol. Chem. **269:**23177–23184.
24. **Lim, K. C., G. Lakshmanan, S. E. Crawford, Y. Gu, F. Grosveld, and J. D. Engel.** 2000. Gata3 loss leads to embryonic lethality due to noradrenaline deficiency of the sympathetic nervous system. Nat. Genet. **25:**209–212.
25. **Ludecke, H. J., J. Schaper, P. Meinecke, P. Momeni, S. Gros, D. von Holtum, H. Hirche, M. J. Abramowicz, B. Albrecht, C. Apacik, H. J. Christen, U. Claussen, K. Devriendt, E. Fastnacht, A. Forderer, U. Friedrich, T. H. Goodship, M. Greiwe, H. Hamm, R. C. Hennekam, G. K. Hinkel, M. Hoeltzenbein, H. Kayserili, F. Majewski, M. Mathieu, R. McLeod, A. T. Midro, U. Moog, T. Nagai, N. Niikawa, K. H. Orstavik, E. Plochl, C. Seitz, J. Schmidtke, L. Tranebjaerg, M. Tsukahara, B. Wittwer, B. Zabel, G. Gillessen-Kaesbach, and B. Horsthemke.** 2001. Genotypic and phenotypic spectrum in tricho-rhino-phalangeal syndrome types I and III. Am. J. Hum. Genet. **68:**81–91.
26. **Malik, T. H., and R. A. Shivdasani.** 2000. Structure and expression of a novel Frizzled gene isolated from the developing mouse gut. Biochem. J. **349:**829–834.
27. **Malik, T. H., S. A. Shoichet, P. Latham, T. Kroll, L. L. Peters, and R. A. Shivdasani.** 2001. Transcriptional repression and developmental functions of the atypical vertebrate GATA protein TRPS1. EMBO J. **20:**1715–1725.
28. **Mallampalli, R. K., M. J. Acarregui, and J. M. Snyder.** 1997. Differentiation of the alveolar epithelium in the fetal lung, p. 119–162. *In* J. A. McDonald (ed.), Lung biology in health and disease, vol. 100. Lung growth and development. Marcel Dekker, New York, N.Y.
29. **Mao, X., Y. Fujiwara, and S. H. Orkin.** 1999. Improved reporter strain for monitoring Cre recombinase-mediated DNA excisions in mice. Proc. Natl. Acad. Sci. USA **96:**5037–5042.
30. **McLeod, M. J.** 1980. Differential staining of cartilage and bone in whole mouse fetuses by alcian blue and alizarin red S. Teratology **22:**299–301.
31. **Millar, S. E.** 2002. Molecular mechanisms regulating hair follicle development. J. Investig. Dermatol. **118:**216–225.
32. **Molkentin, J. D., Q. Lin, S. A. Duncan, and E. N. Olson.** 1997. Requirement of the transcription factor GATA4 for heart tube formation and ventral morphogenesis. Genes Dev. **11:**1061–1072.
33. **Momeni, P., G. Glockner, O. Schmidt, D. von Holtum, B. Albrecht, G. Gillessen-Kaesbach, R. Hennekam, P. Meinecke, B. Zabel, A. Rosenthal, B. Horsthemke, and H. J. Ludecke.** 2000. Mutations in a new gene, encoding a zinc-finger protein, cause tricho-rhino-phalangeal syndrome type I. Nat. Genet. **24:**71–74.
34. **Morrisey, E. E., Z. Tang, K. Sigrist, M. M. Lu, F. Jiang, H. S. Ip, and M. S. Parmacek.** 1998. GATA6 regulates HNF4 and is required for differentiation of visceral endoderm in the mouse embryo. Genes Dev. **12:**3579–3590.
35. **Muller, R., T. Hildebrand, H. J. Hauselmann, and P. Ruegsegger.** 1996. In vivo reproducibility of three-dimensional structural properties of noninvasive bone biopsies using 3D-pQCT. J. Bone Miner. Res. **11:**1745–1750.
36. **Nardelli, J., D. Thiesson, Y. Fujiwara, F. Y. Tsai, and S. H. Orkin.** 1999. Expression and genetic interaction of transcription factors GATA-2 and GATA-3 during development of the mouse central nervous system. Dev. Biol. **210:**305–321.
37. **Narita, N., M. Bielinska, and D. B. Wilson.** 1997. Wild-type endoderm abrogates the ventral developmental defects associated with GATA-4 deficiency in the mouse. Dev. Biol. **189:**270–274.
38. **Nichols, K. E., J. D. Crispino, M. Poncz, J. G. White, S. H. Orkin, J. M. Maris, and M. J. Weiss.** 2000. Familial dyserythropoietic anaemia and

thrombocytopenia due to an inherited mutation in GATA1. Nat. Genet. **24:**266–270.

39. **Olson, E. N., H. H. Arnold, P. W. Rigby, and B. J. Wold.** 1996. Know your neighbors: three phenotypes in null mutants of the myogenic bHLH gene MRF4. Cell **85:**1–4.

40. **Omichinski, J. G., G. M. Clore, O. Schaad, G. Felsenfeld, C. Trainor, E. Appella, S. J. Stahl, and A. M. Gronenborn.** 1993. NMR structure of a specific DNA complex of Zn-containing DNA binding domain of GATA-1. Science **261:**438–446.

41. **Oro, A. E., and M. P. Scott.** 1998. Splitting hairs: dissecting roles of signaling systems in epidermal development. Cell **95:**575–578.

42. **Pandolfi, P. P., M. E. Roth, A. Karis, M. W. Leonard, E. Dzierzak, F. G. Grosveld, J. D. Engel, and M. H. Lindenbaum.** 1995. Targeted disruption of the GATA3 gene causes severe abnormalities in the nervous system and in fetal liver haematopoiesis. Nat. Genet. **11:**40–44.

43. **Pehlivan, T., B. R. Pober, M. Brueckner, S. Garrett, R. Slaugh, R. Van Rheeden, D. B. Wilson, M. S. Watson, and A. V. Hing.** 1999. GATA4 haploinsufficiency in patients with interstitial deletion of chromosome region 8p23.1 and congenital heart disease. Am. J. Med. Genet. **83:**201–206.

44. **Pevny, L., M. C. Simon, E. Robertson, W. H. Klein, S. F. Tsai, V. D'Agati, S. H. Orkin, and F. Costantini.** 1991. Erythroid differentiation in chimaeric mice blocked by a targeted mutation in the gene for transcription factor GATA-1. Nature **349:**257–260.

45. **Reiter, J. F., J. Alexander, A. Rodaway, D. Yelon, R. Patient, N. Holder, and D. Y. Stainier.** 1999. Gata5 is required for the development of the heart and endoderm in zebrafish. Genes Dev. **13:**2983–2995.

46. **Robledo, R. F., L. Rajan, X. Li, and T. Lufkin.** 2002. The Dlx5 and Dlx6 homeobox genes are essential for craniofacial, axial, and appendicular skeletal development. Genes Dev. **16:**1089–1101.

47. **Sauer, B.** 1987. Functional expression of the *cre-lox* site-specific recombination system in the yeast *Saccharomyces cerevisiae*. Mol. Cell. Biol **7:**2087–2096.

48. **Shivdasani, R. A., Y. Fujiwara, M. A. McDevitt, and S. H. Orkin.** 1997. A lineage-selective knockout establishes the critical role of transcription factor GATA-1 in megakaryocyte growth and platelet development. EMBO J. **16:**3965–3973.

49. **Sugiura, Y., M. Shionoya, T. Inoue, and T. Tsuruta.** 1976. Tricho-rhino-phalangeal syndrome: report on three unrelated families. Jpn. J. Hum. Genet. **21:**13–22.

50. **Svensson, E. C., R. L. Tufts, C. E. Polk, and J. M. Leiden.** 1999. Molecular cloning of FOG-2: a modulator of transcription factor GATA-4 in cardiomyocytes. Proc. Natl. Acad. Sci. USA **96:**956–961.

51. **Tevosian, S. G., A. E. Deconinck, A. B. Cantor, H. I. Rieff, Y. Fujiwara, G. Corfas, and S. H. Orkin.** 1999. FOG-2: a novel GATA-family cofactor related to multitype zinc-finger proteins Friend of GATA-1 and U-shaped. Proc. Natl. Acad. Sci. USA **96:**950–955.

52. **Ting, C. N., M. C. Olson, K. P. Barton, and J. M. Leiden.** 1996. Transcription factor GATA-3 is required for development of the T-cell lineage. Nature **384:**474–478.

53. **Tretter, A. E., R. C. Saunders, C. M. Meyers, J. S. Dungan, K. Grumbach, C. C. Sun, A. B. Campbell, and E. A. Wulfsberg.** 1998. Antenatal diagnosis of lethal skeletal dysplasias. Am. J. Med. Genet. **75:**518–522.

54. **Tsai, F. Y., C. P. Browne, and S. H. Orkin.** 1998. Knock-in mutation of transcription factor GATA-3 into the GATA-1 locus: partial rescue of GATA-1 loss of function in erythroid cells. Dev. Biol. **196:**218–227.

55. **Tsai, F. Y., G. Keller, F. C. Kuo, M. Weiss, J. Chen, M. Rosenblatt, F. W. Alt, and S. H. Orkin.** 1994. An early haematopoietic defect in mice lacking the transcription factor GATA-2. Nature **371:**221–226.

56. **Tsang, A. P., J. E. Visvader, C. A. Turner, Y. Fujiwara, C. Yu, M. J. Weiss, M. Crossley, and S. H. Orkin.** 1997. FOG, a multitype zinc finger protein, acts as a cofactor for transcription factor GATA-1 in erythroid and megakaryocytic differentiation. Cell **90:**109–119.

57. **Tybulewicz, V. L., C. E. Crawford, P. K. Jackson, R. T. Bronson, and R. C. Mulligan.** 1991. Neonatal lethality and lymphopenia in mice with a homozygous disruption of the c-*abl* proto-oncogene. Cell **65:**1153–1163.

58. **Van Esch, H., P. Groenen, A. M. Nesbit, S. Schuffenhauer, P. Lichtner, G. Vanderlinden, B. Harding, R. Beetz, R. W. Bilous, I. Holdaway, N. J. Shaw, J. P. Fryns, W. Van de Ven, R. V. Thakker, and K. Devriendt.** 2000. GATA3 haplo-insufficiency causes human HDR syndrome. Nature **406:**419–422.

59. **van Genderen, C., R. M. Okamura, I. Farinas, R. G. Quo, T. G. Parslow, L. Bruhn, and R. Grosschedl.** 1994. Development of several organs that require inductive epithelial-mesenchymal interactions is impaired in LEF-1-deficient mice. Genes Dev. **8:**2691–2703.

60. **Yueh, Y. G., D. P. Gardner, and C. Kappen.** 1998. Evidence for regulation of cartilage differentiation by the homeobox gene Hoxc-8. Proc. Natl. Acad. Sci. USA **95:**9956–9961.

61. **Zhou, Y., K. C. Lim, K. Onodera, S. Takahashi, J. Ohta, N. Minegishi, F. Y. Tsai, S. H. Orkin, M. Yamamoto, and J. D. Engel.** 1998. Rescue of the embryonic lethal hematopoietic defect reveals a critical role for GATA-2 in urogenital development. EMBO J. **17:**6689–6700.

62. **Zhu, J., R. J. Hill, P. J. Heid, M. Fukuyama, A. Sugimoto, J. R. Priess, and J. H. Rothman.** 1997. *end-1* encodes an apparent GATA factor that specifies the endoderm precursor in *Caenorhabditis elegans* embryos. Genes Dev. **11:**2883–2896.